# Ubl4A is required for insulin-induced Akt plasma membrane translocation through promotion of Arp2/3-dependent actin branching

Yu Zhao[a], Yuting Lin[a], Honghong Zhang[a], Adriana Mañas[a], Wenwen Tang[b], Yuzhu Zhang[c], Dianqing Wu[b], Anning Lin[c], and Jialing Xiang[a,1]

[a]Department of Biology, Illinois Institute of Technology, Chicago, IL 60616; [b]Department of Pharmacology, Yale University School of Medicine, New Haven, CT 06520; and [c]Ben May Department for Cancer Research, University of Chicago, Chicago, IL 60637

Edited by Melanie H. Cobb, University of Texas Southwestern Medical Center, Dallas, TX, and approved July 1, 2015 (received for review May 6, 2015)

**The serine-threonine kinase Akt is a key regulator of cell proliferation and survival, glucose metabolism, cell mobility, and tumorigenesis. Activation of Akt by extracellular stimuli such as insulin centers on the interaction of Akt with PIP3 on the plasma membrane, where it is subsequently phosphorylated and activated by upstream protein kinases. However, it is not known how Akt is recruited to the plasma membrane upon stimulation. Here we report that ubiquitin-like protein 4A (Ubl4A) plays a crucial role in insulin-induced Akt plasma membrane translocation. Ubl4A knockout newborn mice have defective Akt-dependent glycogen synthesis and increased neonatal mortality. Loss of Ubl4A results in the impairment of insulin-induced Akt translocation to the plasma membrane and activation. Akt binds actin-filaments and colocalizes with actin-related protein 2 and 3 (Arp2/3) complex in the membrane ruffles and lamellipodia. Ubl4A directly interacts with Arp2/3 to accelerate actin branching and networking, allowing Akt to be in close proximity to the plasma membrane for activation upon insulin stimulation. Our finding reveals a new mechanism by which Akt is recruited to the plasma membrane for activation, thereby providing a missing link in Akt signaling.**

Ubl4A | Akt translocation | Arp2/3 complex | actin branching | insulin

The serine-threonine kinase Akt (also known as protein kinase B) is a key regulator of cell proliferation and survival, glucose metabolism, cell mobility, and tumorigenesis, and its dysregulation has been implicated in human diseases (1–3). Akt is activated by a variety of extracellular stimuli including insulin (4). Upon stimulation, Akt is recruited to the plasma membrane by phosphatidylinositol (3-5)-triphosphate (PIP3), which interacts directly with the Akt pleckstrin homology (PH) domain, and is subsequently phosphorylated at Thr308 and Ser473, and thus activated, by protein kinases such as phosphoinositide-dependent kinase-1 (PDK1) and mammalian target of rapamycin (mTOR) complex 2 (mTORC2) (5–8). It is, however, not known how Akt translocates to the plasma membrane in response to extracellular signals such as insulin.

Ubl4A (also known as Gdx in mammalian or Get5 in yeast) is a small ubiquitin-like protein encoded by an X-linked housekeeping gene (9). Although Ubl4A contains an ubiquitin-like domain at its N terminus, it lacks ubiquitination activity (10). In yeast, Ubl4A homolog Get5 forms a complex with Get4 to assist Get3 for recruitment of nascent synthesized tail-anchored (TA) proteins and their delivery to the endoplasmic reticulum (11, 12). Ubl4A and other mammalian Get homologs are also involved in the recruitment and delivery of TA protein into the endoplasmic reticulum membrane (11, 13). Furthermore, Ubl4A can also suppress tumorigenesis through regulation of signal transducer and activation of transcription 3 (13) and is involved in DNA damage-mediated cell death (14). Here we report that Ubl4A is required for insulin-induced Akt plasma membrane translocation and activation through direct promotion of Arp2/3-dependent actin branching, thereby playing a critical role in regulation of glycogen synthesis for neonatal survival.

## Results

**Ubl4A-Deficient Mice Display Increased Neonatal Mortality and a Defect in Liver Glycogen Synthesis.** To better understand the biological functions of Ubl4A, we generated Ubl4A-deficient mice (Fig. S1). Ubl4A knockout (KO) mice were viable but displayed increased neonatal mortality (occurring mostly within 24 h after birth) compared with their wild type (WT) littermates (Fig. 1*A*). We noticed that some Ubl4A KO pups displayed signs of cyanosis before death (Fig. 1*A*, *Inset*). The surviving Ubl4A KO newborns, however, appeared to be normal despite modestly low body weight (Fig. 1*B*). We wondered that increased mortality of Ubl4A KO neonates might be the result of defective glucose homeostasis, as glycogenolysis and mobilization of glycogen storage from liver are vital for the newborns to combat starvation-induced hypoglycemia (15). Indeed, glycogen staining analysis revealed that WT neonatal livers had typical abundant accumulation of glycogen ∼5 h after birth (Fig. 1 *C* and *D*), which was quickly consumed 10 h after birth (Fig. S2). In contrast, glycogen synthesis was significantly lower in Ubl4A KO livers than in WT livers during the same period (Fig. 1 *C* and *D*). Consistently, phosphorylation of liver glycogen synthase (GS), which is an effector in the Akt-GS kinase 3β (GSK3β) pathway (16), was increased in the primary KO hepatocytes compared with the WT counterparts (Fig. 1*E*), suggesting the activity of GS was decreased. Furthermore, the inhibitory phosphorylation of GSK3β, which is the upstream kinase of GS, was decreased in the Ubl4A KO hepatocyte cells (Fig. 1*E*). Thus, the defect in liver glycogen synthesis may contribute to, at least in part, the increased neonatal mortality and growth retardation in Ubl4A-deficient mice.

### Significance

**The signal-induced Akt membrane recruitment is a crucial step for its activation, but the underlying mechanism is incompletely understood. We show that ubiquitin-like protein 4A (Ubl4A) is required for insulin-induced Akt membrane translocation through direct promotion of actin-related protein 2 and 3 (Arp2/3)-dependent actin branching, thereby ensuring glycogen synthesis for neonatal survival. As a novel Arp2/3-binding protein, Ubl4A may play important roles in the translocation of other actin-binding molecules controlled by a similar mechanism, as well as a broad range of cellular functions related to the actin branching network.**

Author contributions: Y. Zhao, D.W., and J.X. designed research; Y. Zhao, Y.L., H.Z., A.M., W.T., and Y. Zhang performed research; Y. Zhao, Y.L., D.W., A.L., and J.X. analyzed data; and Y. Zhao, D.W., A.L., and J.X. wrote the paper.

The authors declare no conflict of interest.

This article is a PNAS Direct Submission.

[1]To whom correspondence should be addressed. Email: xiang@iit.edu.

This article contains supporting information online at www.pnas.org/lookup/suppl/doi:10.1073/pnas.1508647112/-/DCSupplemental.

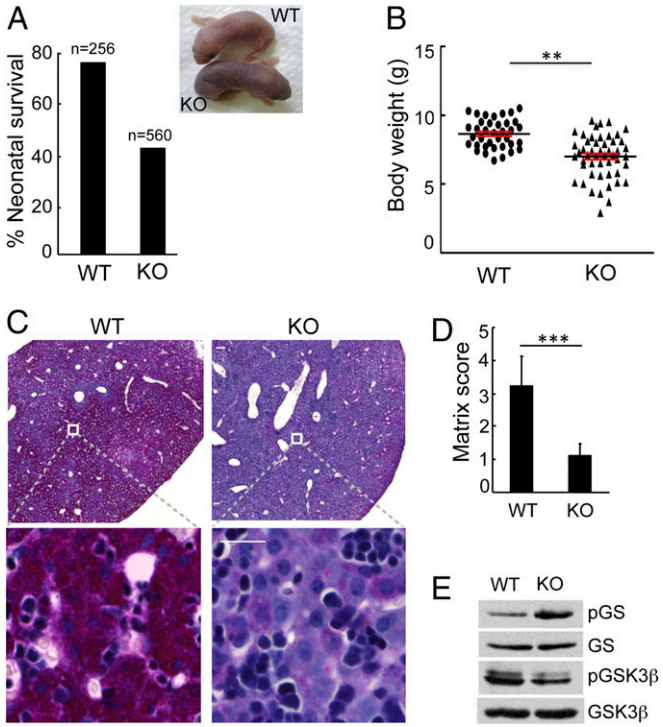


**Fig. 1.** Ubl4A-deficient mice display increased neonatal mortality and a defect in liver glycogen synthesis. (*A*) The survival rate of neonates within 24 h after birth. (*Inset*) Representative WT and KO littermates ∼5 h after birth. (*B*) The body weight of 3-wk-old mice; data shown are mean ± SEM. WT, $n = 37$; KO, $n = 50$. $^{**}P < 0.01$. (*C*) Liver glycogen PAS staining of the neonates ∼5 h after birth. (Scale bar, 100 μm.) (*D*) Quantitative analysis of liver PAS staining by matrix score. The average percentage of PAS positive area is scored as 0 (0%), 1 (25%), 3 (75%), or 4 (100%). Error bars present SD. $n = 9$. $^{***}P < 0.001$. (*E*) Immunoblotting analysis of phosphorylated and total GSK3β and GS of primary hepatocytes.

**Loss of Ubl4A Results in Impaired Akt Plasma Membrane Translocation and Activation.** The defect in glycogen synthesis in Ubl4A KO mice led us to investigate activation of the GSK3β upstream apical kinase Akt. Insulin-induced Akt phosphorylation at Ser473 and Thr308, both of which are required for Akt activation on the plasma membrane (17), was significantly decreased in Ubl4A KO primary hepatocytes and mouse embryonic fibroblasts (MEFs) compared with their WT counterparts (Fig. 2*A*). As expected, phosphorylation of S6K, an Akt substrate, was impaired in Ubl4A-deficient MEFs (Fig. S3*A*). In contrast, Akt phosphorylation at Thr450, which is involved in stabilization of newly synthesized Akt in the cytoplasm (18), was not affected (Fig. S3*B*). The impaired activation of Akt could be a result of defects either in Akt translocation from the cytoplasm to the plasma membrane or in its upstream components such as PIP3, mTOR, or PDK1 on the plasma membrane. The latter is unlikely. There was no significant difference in production of PIP3 between insulin-treated WT and KO fibroblasts (Fig. 2*B* and Fig. S3*C*). Consistently, the addition of exogenous PIP3 to the KO MEFs also failed to rescue Akt activation in response to insulin stimulation (Fig. 2*C*). Furthermore, insulin-induced activation of mTOR and its enzymatic activity were not affected by loss of Ubl4A (Fig. S3 *D* and *E*), and translocation and activation of PDK1 were only marginally reduced in Ubl4A KO MEFs (Fig. S3*F*). In contrast, loss of Ubl4A, which resulted in the reduction of the membrane Thr308- and Ser473-phosphorylated Akt, reduced total endogenous Akt proteins on the membrane (Fig. 2*D*). Interestingly, translocation and activation of Akt to other major cellular compartments, such as mitochondria and nucleus (19, 20), were not significantly affected (Fig. 2*D*). This notion is further supported by the significant reduction of phosphorylated endogenous Akt on the plasma membrane in Ubl4A KO cells, as analyzed using confocal microscope imaging (Fig. 2 *E* and *F*). Thus, loss of Ubl4A mainly affects Akt plasma membrane translocation.

**Regulation of Akt Membrane Translocation by Ubl4A Depends on the Actin Network and the Arp2/3 Complex.** To determine how Ubl4A regulates the translocation of Akt from the cytoplasm to the plasma membrane, a step about which very little is known, WT and KO primary fibroblasts were transfected with expression vector-encoding GFP-tagged Akt-PH domain (Akt-PH-GFP). Time-lapse microscopy revealed that upon insulin stimulation, Akt-PH-GFP proteins formed actin filament-like structures and appeared to be more readily recruited to the plasma membrane-ruffling regions in WT than in Ubl4A-deficient fibroblasts (Fig. 3*A* and Movies S1 and S2). Because Akt-PH-GFP seemed to be more extensively recruited to the structures similar to actin filaments and subsequently accumulated in membrane-ruffling regions (Fig. 3*A*), we examined the colocalization of F-actin and Akt-PH-GFP upon insulin stimulation. Confocal immunofluorescence microscopy revealed that Akt-PH-GFP proteins indeed

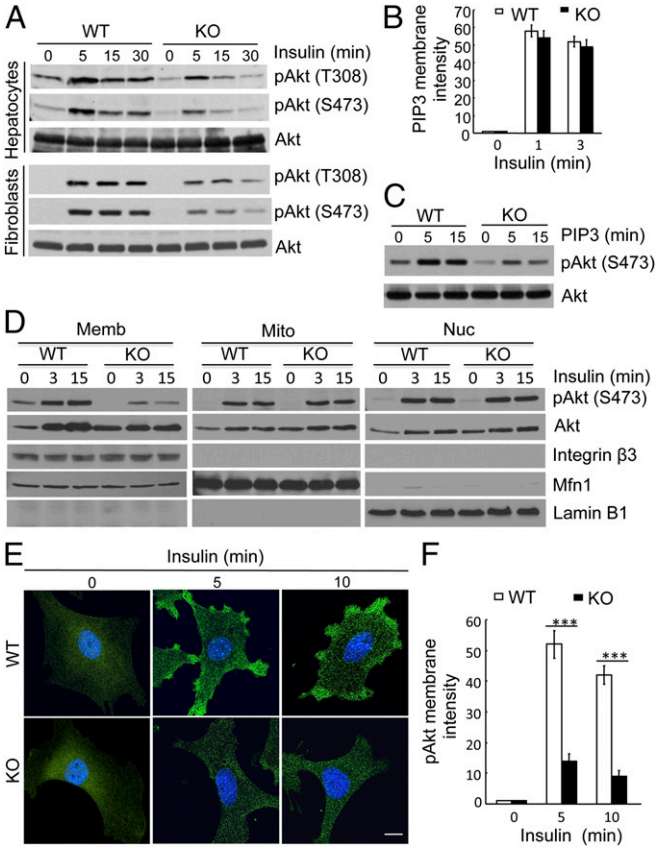


**Fig. 2.** Loss of Ubl4A results in impaired Akt plasma membrane translocation and activation. (*A*) Activation of Akt in primary hepatocytes and MEFs stimulated with insulin (2 μg/mL) for various times indicated. (*B*) Density quantitation of PIP3 in primary MEFs stimulated with insulin and immunostained using anti-PIP3 antibody (Fig. S3*C*). Error bars present SD. $n = 30$ cells per group. (*C*) Activation of Akt in WT and KO MEFs treated with or without exogenous PIP3 (100 μM) for the times indicated. (*D*) Immunoblots of cellular fractionations of plasma-rich membrane (Memb), mitochondria rich (Mito), or nucleus rich (Nuc) for endogenous phosphorylated and total Akt in WT and KO MEFs stimulated with or without insulin. (*E*) Cellular localizations of endogenous pAkt (S473) in WT and KO MEFs. (Scale bar, 10 μm.) (*F*) Membrane density analysis of pAkt shown in *E*. Error bars present SD. $n = 65$ cells per group. $^{***}P < 0.001$.

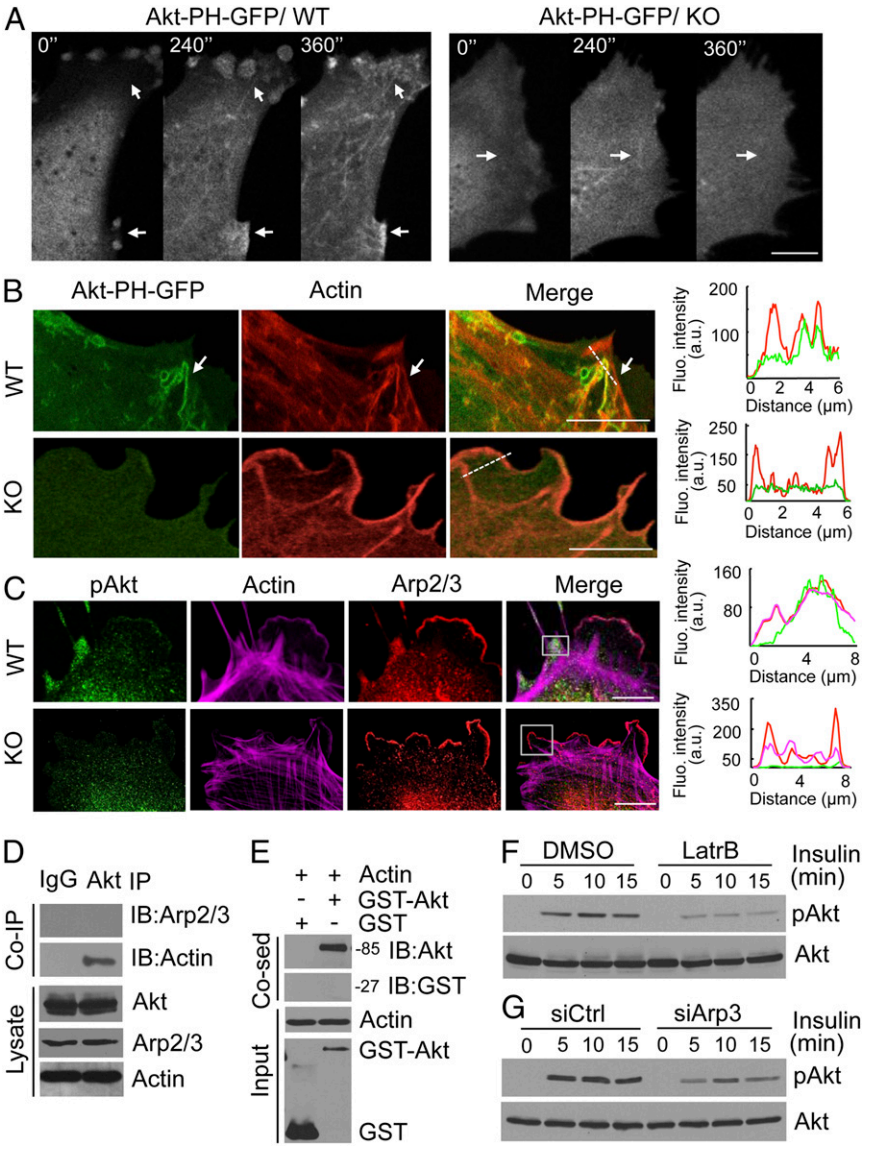


**Fig. 3.** Ubl4A-mediated Akt activation depends on actin network and the Arp2/3 complex in membrane ruffles and lamellipodia. (*A*) Snapshots of time-lapse movies show that Akt-PH-GFP formed actin filament-like structures and translocated to the plasma membrane upon insulin stimulation. (Scale bar, 10 μm.) (*B*) Colocalization between transfected Akt-PH-GFP and actin. The images show a portion of membrane region of individual cells. (*Inset*) Line scan of fluorescence intensity. (Scale bar, 10 μm.) (*C*) Colocalization among endogenous pAkt, actin, and Arp2/3 in WT and KO MEFs treated with insulin. (*Inset*) Line scan of fluorescence intensity. (Scale bar, 10 μm.) (*D*) Immunoprecipitation with anti-Akt antibody in combination with immunoblotting with anti-Arp3 and anti-actin antibodies. Input, one tenth of cell lysates. (*E*) Cosedimentation (Co-sed) assay of F-actin filaments with purified GST-Akt. (*F* and *G*) Activation of Akt in WT MEFs treated with or without actin polymerization inhibitor LatrB (2.5 μM) (*F*), or transfected with Arp3 siRNA (siArp3) (*G*). Validation of Arp3 knockdown was shown in Fig. S4*B*.

colocalized with F-actin filaments in WT, but not in the Ubl4A-deficient fibroblasts (Fig. 3*B*). Consistently, phosphorylated endogenous Akt was also colocalized with actin in the plasma membrane, especially in membrane ruffles and lamellipodia in WT fibroblasts (Fig. 3*C*). Interestingly, phosphorylated endogenous Akt was well colocalized with actin-related protein complex Arp2/3, which is essential for actin branching underneath the plasma membrane (21, 22) in the same regions (Fig. 3*C*). The colocalization of phosphorylated endogenous Akt with actin and Arp2/3 on the plasma membrane was significantly reduced in Ubl4A-deficient MEFs (Fig. 3*C*). In addition, Akt interacted only with actin, especially F-actin filaments, but not Arp2/3, as determined by coimmunoprecipitation and cosedimentation (Fig. 3 *D* and *E*). Furthermore, the Ubl4A-dependent colocalization of Akt with actin and Arp2/3 upon stimulation appeared to involve in Akt activation, as treatment of primary MEFs with F-actin inhibitor Latrunculin B (LatrB) (23), an Arp2/3 inhibitor (CK666) (24), or Arp3 siRNA abrogated insulin-induced Akt activation (Fig. 3 *F* and *G* and Fig. S4). These results indicate that actin and the Arp2/3 complex are critical for Ubl4A-mediated Akt translocation to the plasma membrane for activation.

**Ubl4A Directly Interacts with Arp2/3 and Thereby Accelerates Arp2/3-Dependent Actin Nucleation.** The observations that both actin and Arp2/3 are critical for Ubl4A-mediated Akt activation led us to test whether Ubl4A regulated Arp2/3-dependent actin branching, thereby bringing Akt in close proximity to the plasma membrane for activation. First, we analyzed the cellular localization of Ubl4A and Arp2/3 proteins. Confocal immunofluorescence microscopy revealed that Ubl4A indeed colocalized with Arp2/3 in membrane ruffles and lamellipodia (Fig. 4*A*). To further determine whether there was a physical interaction between

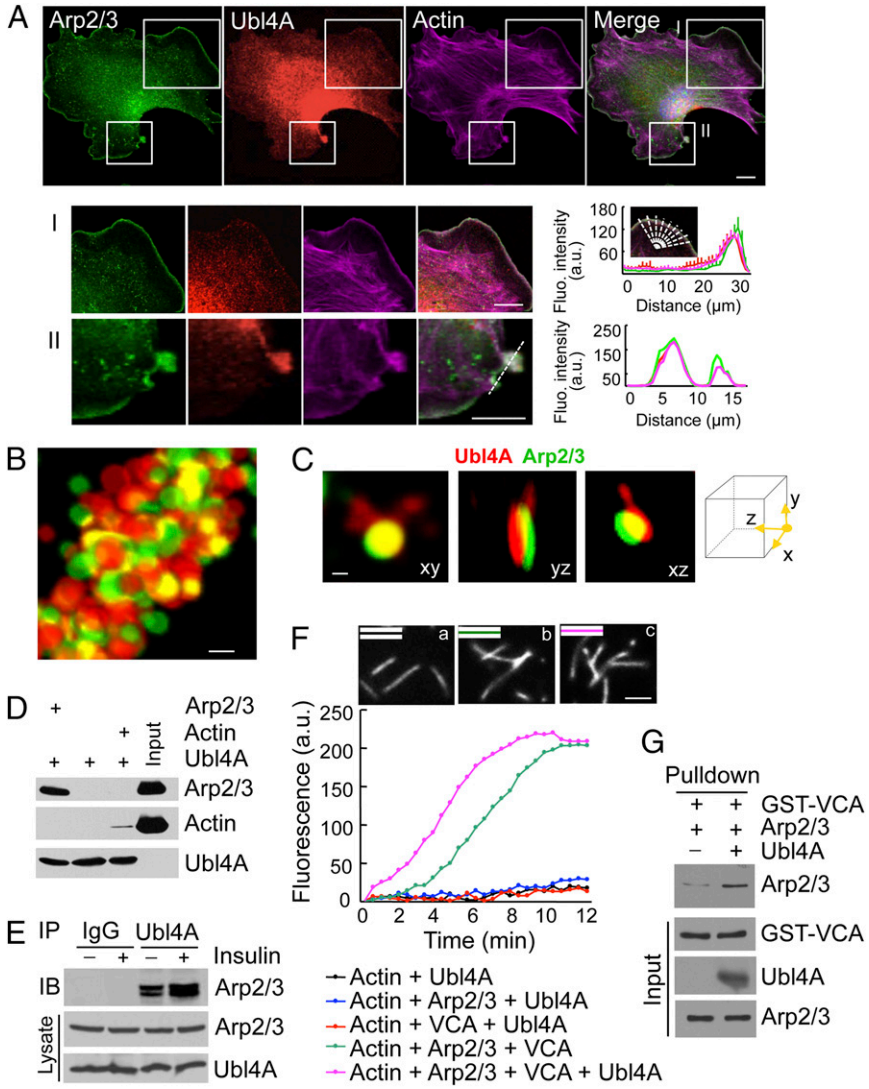


**Fig. 4.** Ubl4A directly interacts with Arp2/3 and promotes Arp2/3-dependent actin branching nucleation. (*A*) Colocalization between endogenous Ubl4A and Arp2/3 in WT fibroblasts upon insulin stimulation. (Scale bar, 10 μm.) (*Lower*) Enlarged boxed areas from regions I and II. (*Inset*) Quantitation of multiple-line (region I, error bars present SD, nine line scans) or single-line (region II) scans. (*B*) GSD-3D imaging of immunostained endogenous Ubl4A (red) and Arp2/3 (green). (Scale bar, 0.1 μm.) (*C*) A zoom-in view of a cross-section of individual molecule of *B* shows 3D direct interaction between Ubl4A and Arp2/3. (Scale bar, 10 nm.) (*D*) Pulldown assay using purified His-Ubl4A, actin, and Arp2/3 proteins. (*E*) Coimmunoprecipitation assay for Ubl4A and Arp2/3. (*F*) Actin polymerization assay (*Bottom*) and actin branching imaged by TIRF microscopy using anti-stain 488-phalloidin-labeled actin (*Top*). (Scale bar, 5 μm.) (*G*) Pulldown assay for GST-VCA and immunoblot with anti-Arp3 antibody.

Ubl4A and the Arp2/3 complex, the 3D localizations of individual Ubl4A and Arp2/3 protein molecules were visualized using a super resolution microscope based on ground state depletion (GSD) (Fig. 4 *B* and *C*); the results demonstrate that Ubl4A interacts directly with Arp2/3. Consistently, pulldown assay using recombinant His-tagged Ubl4A and purified Arp2/3 proteins also showed that Ubl4A specifically interacts with Arp2/3 (Fig. 4*D*). Importantly, the interaction between endogenous Ubl4A and the Arp2/3 complex could be further augmented by insulin (Fig. 4*E*). These data suggest there is a regulatable physical interaction between Ubl4A and Arp2/3 in response to extracellular signals.

Next, we determined whether physical interaction of Ubl4A with the Arp2/3 complex influences the actin nucleated branching process. In vitro actin polymerization assay showed that addition of Ubl4A alone has no detectable effect on actin assembly (Fig. 4*F, a*, Actin+Ubl4A). The actin branch nucleation can be initiated by Arp2/3 in the presence of VCA (verprolin, cofilin, acidic), a domain of WASP protein (Wiskott–Aldrich syndrome protein). VCA is known to be essential for Arp2/3-dependent actin nucleation (25–27) (Fig. 4*F, b*, Actin+Arp2/3+VCA). Importantly, Ubl4A was able to further promote Arp2/3-VCA-dependent actin branching (Fig. 4*F, c*, Actin+Ubl4A+Arp2/3+VCA). However, Ubl4A could not replace the role of VCA in activation of Arp2/3 (Fig. 4*F*, Actin+Ubl4A+Arp2/3). Instead, the interaction between Arp2/3 and VCA was further accelerated in the presence of Ubl4A (Fig. 4*G*). Taken together, this indicates that Ubl4A promotes actin branching through direct association with the Arp2/3 complex, thereby facilitating Arp2/3 interaction with VCA for actin nucleation upon insulin stimulation.

## Discussion

A key step in Akt activation is its translocation from the cytoplasm to the plasma membrane, where it interacts with PIP3 through the Akt PH domain and is subsequently activated by upstream protein kinases including PDK1 and mTORC2 (7, 8). How Akt translocates from the cytosol to the plasma membrane

is not known, even though it has been thought that passive diffusion might be involved. Our data clearly demonstrate that Ubl4A is crucial for insulin-induced Akt activation through promotion of an Arp2/3-mediated actin network underneath the plasma membrane, especially in the regions of membrane ruffles and lamellipodia.

The actin network (meshwork) underneath the plasma membrane, especially in lamellipodia and membrane ruffles, plays a crucial role in many important cellular events (28, 29). Here we show that the actin network is also important for membrane translocation of Akt in response to insulin. This conclusion is supported by the following evidence. First, upon stimulation by insulin, Akt translocated to the plasma membrane, clustered in lamellipodia and membrane ruffles (Figs. 2*E* and 3*C*), consistent with previous reports (30). Second, Akt associated with actin, especially F actin filaments (Fig. 3 *D* and *E*), which is also consistent with previous findings (31, 32). Third, Akt colocalized with the Arp2/3 complex in membrane ruffles, although it did not bind to Arp2/3 (Fig. 3 *C* and *D*). Fourth, Arp2/3 complex-dependent actin branching is known to be essential for the formation of lamellipodia and membrane ruffles (22, 29). Inhibition of either Arp2/3 or the actin network abolished Akt membrane translocation and activation (Fig. 3 *F* and *G*). Finally, Ubl4A directly associated with the Arp2/3 complex and accelerated the interaction between Arp2/3 and VCA (Fig. 4*G*) for actin nucleation and branching (Fig. 4*F*). Together, our data support a model in which Ubl4A-mediated actin branching underneath the plasma membrane brings Akt in proximity to interact with the plasma membrane and undergo subsequent activation.

Our results show that the PH domain of Akt appears to be a minimal requirement for Akt to bind actin and membrane translocation in response to insulin (Fig. 3*A*), consistent with the previous report that the Akt PH domain directly interacts with actin (33). It is likely that in addition to Akt, Ubl4A-Arp2/3-mediated actin branching may be involved in signal-induced translocation of some other PH domain-containing proteins. Ubl4A-Arp2/3-mediated actin branching is also likely to have broad significance beyond growth factor-induced responses in hepatocytes and fibroblasts. Akt activation by fMLP (N-formyl-Met-Leu-Phe), which signals through G protein-coupled receptor, was also impaired in Ubl4A KO neutrophils (Fig. S5*A*). It is anticipated that Ubl4A may play important roles in a broad range of cellular functions related to actin cytoskeletal reorganization, given its role in promotion of Arp2/3-dependent actin filament branching. In fact, mouse neutrophils lacking Ubl4A showed significant directionality defects during chemotaxis (Fig. S5*B*), a process in which actin cytoskeletal reorganization has a key role. It is possible that Ubl4A-Arp2/3 may underlie a general mechanism for membrane translocation of other signaling molecules in response to extracellular stimulations. This needs to be addressed in future studies.

## Methods

**Mice and Primary Cell Culture.** All animal studies were performed in accordance with guidelines of the Institutional Animal Care and Use Committee. The Ubl4A KO mice were generated by Taconic (Artemis Pharmaceuticals Ltd.), using a Cre/loxP-Rosa26 deleter system. In brief, *Ubl4A* is on the X chromosome and contains four exons, and exons 2, 3, and 4 were deleted through flanking with two loxP sites by the Cre recombinase (Fig. S1). The $Ubl4A^{flox/y}$ male mice were crossed with rosa26 (SA-CrepA) mice to generate Cre/$Ubl4A^{-/y}$. The Cre transgene was deleted by crossing male Cre/$Ubl4A^{-/y}$ with female $Ubl4A^{flox/+}$ and $Ubl4A^{+/-}$ mice. The KO homozygous mice were obtained by breeding $Ubl4A^{-/+}$ and male $Ubl4A^{-/y}$ mice. $Ubl4A^{-/-}$ mice were maintained as homozygotes on the C57BL/6 genetic background. MEFs were isolated from E14 (embryonic day 14) mouse embryos and used for experiments within five passages. Primary hepatocytes were isolated from 4-wk-old mice, and primary neutrophils were isolated from bone marrows of 6–8-wk-old mice and cultured as described previously (34, 35).

**Glycogen Staining.** Livers and hearts were harvested from newborn pups 3–10 h postbirth. Glycogen was stained using a standard Periodic acid–Schiff (PAS) method in the Pathology Facility at the University of Chicago.

**Immunoblotting.** Cells were lysed in Nonidet P-40 buffer (145 mM NaCl, 5 mM $MgCl_2$, 25 mM Hepes at pH 7.4, 1 mM EDTA, 1 mM EGTA, 1 mM DTT, 0.2% Nonidet P-40), plus a mixture of protease inhibitors including 10 μg/mL leupeptin, 10 μg/mL aprotinin, 10 mM NaF, and 2 mM sodium orthovanadate. Equal amounts of proteins were separated by standard SDS/PAGE and transferred to PVDF membrane. The antibodies against phospho-Akt (Ser473), phospho-Akt (Thr308), phospho-Akt (Thr450), Akt, phospho-p70 S6 Kinase (Thr389), p70 S6 Kinase, phospho-GSK3β, GSK3β, phospho-Glycogen Synthase (pGS, Ser641), Arp3, phospho-mTOR (Ser2448), and mTOR were purchased from Cell Signaling. Antibodies against GS and Ubl4A were purchased from Sigma. Representative results obtained from at least three independent experiments are presented.

**Cellular Fractionation.** Ten culture dishes (100 mm) of primary MEFs (<five passages) were used for each experimental group. Cells were placed in serum-free plain medium for 3 h and then treated with or without insulin (2 μg/mL) for 3 min, followed immediately by washing with ice-cold PBS. Cell pellets were resuspended with 500 μL ice-cold homogenization buffer (20 mM Hepes at pH 7.4, 10 mM NaCl, 1.5 mM $MgCl_2$, 1 mM EDTA, 1 mM EGTA, 1 mM DTT), plus a mixture of protease inhibitors. Cells were homogenized by 30–60 passes through a 27-gauge needle until ∼90% of the cells were broken. Nuclear fractions were obtained by centrifuging at 700 × *g* for 10 min at 4 °C. The plasma membrane-rich fraction was isolated using a Mem-PER Plus Membrane Protein Extraction kit (Life Technologies), and the mitochondrial-rich fraction was isolated using a Mitochondria Fractionation kit (BioVision), all according to the manufacturers' instructions. Integrin β3 was used as a marker for the plasma membrane, Mfn1 (mitochondrial fusion protein 1) for mitochondria, and Lamin B1 for nucleus.

**Purification of Recombinant Ubl4A Protein.** Murine full-length Ubl4A DNA was cloned into vector pET-14b between the NdeI and *Bam*H1 sites with a N-terminal His-tag and transformed into *Escherichia coli* BL21(DE3). Expression of the recombinant proteins was induced with 1 mM isopropyl-β-D-1-thio-galactopyranoside for 4 h at 37 °C. Cells were collected by centrifugation and resuspended in Ni-binding buffer (buffer NB; 20 mM phosphate at pH 7.4, 40 mM imidazole, 500 mM NaCl) plus 1 mM PMSF and 1 mM benzamidine. The samples were sonicated, followed by centrifugation. The cleared supernatant was collected and loaded onto a His-Tap HP column (TGE Heath Care). The column was washed with 91% (vol/vol) buffer NB plus 9% of the Ni-elution buffer (1 M imidazole). The sample was eluted with 50% (vol/vol) buffer NB and 50% Ni-elution buffer and dialyzed in to a 20 mM phosphate buffer containing 500 mM NaCl and 10 mM DTT before use for the experiments.

**Coimmunoprecipitation and Immunocomplex Kinase Assay.** Primary MEFs (<five passages) were harvested and lysed on ice in a lysis buffer containing 20 mM Hepes at pH 7.4 and 1% CHAPS, plus a mixture of protease inhibitors for 30 min. Precleared cell lysates were incubated with protein A/G beads precoated with proper antibodies indicated in the text overnight at 4 °C. The beads were then washed and the immunocomplexes subjected to immunoblotting analysis. The immunocomplex kinase assay was performed as described previously (36), in which mTOR was immunoprecipitated by anti-mTOR antibody and validated by immunoblotting of Rictor, a component of mTORC2. The mRORC2 immunocomplex was incubated for 10 min at 30 °C with purified unactive (unphorsphorylated) Akt protein (1 μg; Millipore) in a kinase reaction buffer containing nonradioactive ATP (100 μM). The phosphorylation of Akt was analyzed by immunoblotting using anti-pAkt (S473) antibody.

**Actin Cosedimentation Assay.** G-actin monomers were prepared from pyrene-labeled rabbit muscle actin (Cytoskeleton Inc.) in G-buffer according to the manufacturer's instruction. Actin (G-actin, 5 μg) was polymerized in polymerization buffer (150 μL) containing purified GST or GST-Akt (1 μg; Sigma-Aldrich) at room temperature for 1 h. F-actin filaments were obtained by ultracentrifugation for 20 min at 150,000 × *g* and subjected to immunoblotting.

**Pulldown Assay.** For His-tag pulldown, purified recombinant full-length His-tagged Ubl4A proteins (3 μg) were incubated for 30 min at 4 °C with 30 μL of nickel-charged agarose beads [preblocked with 5% (wt/vol) BSA] in 300 μL binding buffer (20 mM Tris·HCl at pH 8.0, 500 mM NaCl, 5 mM imidazole). The beads were washed three times with washing buffer (20 mM Tris·HCl at pH 8.0, 500 mM NaCl, 60 mM imidazole). The Ubl4A-Ni beads were mixed with

300 μL binding buffer containing purified actin (20 μg; Cytoskeleton, Inc.) and Arp2/3 complex (10 μg; Cytoskeleton, Inc.), and then the mixture was incubated for 2 h at 4 °C. For the GST pulldown assay, the GST-VCA domain of WASP (160 nM) was incubated with Arp2/3 complex (10 nM) in polymerization buffer (5 mM Tris·HCl at pH 7.5, 50 mM KCl, 2 mM $MgCl_2$, 1 mM EGTA, 0.1 mM $CaCl_2$, 0.3 mM ATP, 0.5 mM DTT) with or without purified Ubl4A (100 μM) for 5 min at 37 °C. GST-VCA and its associated proteins were collected by glutathione beads. The beads were washed three times and subjected to immunoblotting analysis.

**Actin Polymerization Assay and TIRF Imaging.** The actin polymerization assay was performed according to the manufacturer's instruction (Cytoskeleton Inc.). Briefly, the reaction was initiated in an actin polymerization buffer (5 mM Tris·HCl at pH 7.5, 50 mM KCl, 2 mM $MgCl_2$, 1 mM EGTA, 0.1 mM $CaCl_2$, 0.3 mM ATP, 0.5 mM DTT) containing pyrene-labeled rabbit muscle actin (0.8 μM G-actin), 10 nM Arp2/3 complex, and 160 nM GST-VCA either with or without Ubl4A (100 μM). Pyrene fluorescence signals were monitored using a Spectra Max GEMINI EM Spectrofluorometer (Molecular Devices) at 37 °C, with excitation and emission at 350 and 405 nm, respectively. For visualization of actin polymers, the reaction mixture was diluted 50-fold with the polymerization buffer containing 70 nM Anti-stain 488 phalloidin (Cytoskeleton). The images were captured using a TIRF microscope with 160×/1.43 oil HCX PL APO objective.

**Confocal Microscopy and GSD-3D Imaging.** Primary MEFs (<five passages) were grown on 0.1% gelatin-coated glass coverslips placed in a 6-well plate. Cells were deprived of serum for 3 h and then treated with insulin (2 μg/mL) for various times, as indicated. Cells were fixed by 4% (wt/vol) paraformaldehyde for 20 min, permeabilized with 0.3% Triton X-100 in PBS for 15 min, and incubated with primary antibodies indicated in the text for 1 h at room temperature. After incubation for 45 min with the Alexa fluor-conjugated secondary antibodies and fluorescent-labeled Phalloidin for actin staining, the slides were washed and mounted in Prolong Gold Antifade mounting medium (Life Technology) with DAPI for nuclear staining. Immunofluorescence images were captured using a Leica SP5-II-AOBS Tandem Scanner confocal microscope equipped with Leica LAS-AF software. The fluorescence intensities were quantitated by single-line or radial lines scan analysis by ImageJ. For GSD imaging, cells were postfixed with 4% paraformaldehyde for 15 min before imaging to prevent dissociation of secondary antibodies. Slides were embedded with freshly prepared 20 mM β-mercaptoethylamine (Sigma) and imaged using a Leica GSD-3D microscope with a 160×/1.43 oil HCX PL APO objective and an Andor-DU897 BV-7849 camera.

**Time-Lapse Movie.** Primary MEFs were seeded onto 35-mm poly-D-lysine-coated glass bottom microwell dishes and transfected with an Akt-PH-GFP construct (Addgene plasmid 18836) for 16 h, followed by starvation and insulin treatment as described earlier. Time-lapse movies were recorded at 10-s intervals for 10 min in a heated chamber at 37 °C, using a Marianas fluorescence confocal microscope with a 488-nm solid-state laser.

**Neutrophil Chemotaxis Assay.** The chemotaxis assay using a Dunn chamber was carried out as previously described (37), with some modifications (34, 38). Both WT and Ubl4A-deficient neutrophils were simultaneously labeled with different tracing dyes. The experimental labeled groups were alternated in the study to completely eliminate the possibility of any influence from the dye. In addition, the chemoattractant gradients were monitored by using free fluorescein isothiocyanate dye. Only cells under similar gradients were analyzed, using the formula described previously (39), to calculate average directional error, average turning angle, and motility. Time-lapse image series were acquired at 30-s intervals for 30 min.

**Statistical Analysis.** Data were analyzed using ImageJ 1.48 and GraphPad Prism 5 software packages. Significance was determined using two-way ANOVA or a two-tailed *t* test. *P* values less than 0.05 were considered significant, and the level of significance was indicated as $*P < 0.05$, $**P < 0.01$, and $***P < 0.001$.

**ACKNOWLEDGMENTS.** We thank Xiaoyang Wu at the University of Chicago for critical reading of the manuscript and constructive discussion, and the staff in the Microscopy Core Facility at the University of Chicago for technical support for all imaging. This project is partially supported by NIH Grants CA128114 (to J.X.), GM095313 (to A.L.), and HL108430 (to D.W.).

1. Downward J (2004) PI 3-kinase, Akt and cell survival. *Semin Cell Dev Biol* 15(2): 177–182.
2. Hemmings BA, Restuccia DF (2012) PI3K-PKB/Akt pathway. *Cold Spring Harb Perspect Biol* 4(9):a011189.
3. Plas DR, Thompson CB (2005) Akt-dependent transformation: There is more to growth than just surviving. *Oncogene* 24(50):7435–7442.
4. Lawlor MA, Alessi DR (2001) PKB/Akt: A key mediator of cell proliferation, survival and insulin responses? *J Cell Sci* 114(Pt 16):2903–2910.
5. Manning BD, Cantley LC (2007) AKT/PKB signaling: Navigating downstream. *Cell* 129(7):1261–1274.
6. Franke TF (2008) Intracellular signaling by Akt: Bound to be specific. *Sci Signal* 1(24):pe29.
7. Alessi DR, et al. (1997) 3-Phosphoinositide-dependent protein kinase-1 (PDK1): Structural and functional homology with the Drosophila DSTPK61 kinase. *Curr Biol* 7(10):776–789.
8. Facchinetti V, et al. (2008) The mammalian target of rapamycin complex 2 controls folding and stability of Akt and protein kinase C. *EMBO J* 27(14):1932–1943.
9. Toniolo D, Persico M, Alcalay M (1988) A "housekeeping" gene on the X chromosome encodes a protein similar to ubiquitin. *Proc Natl Acad Sci USA* 85(3):851–855.
10. Xu Y, Cai M, Yang Y, Huang L, Ye Y (2012) SGTA recognizes a noncanonical ubiquitin-like domain in the Bag6-Ubl4A-Trc35 complex to promote endoplasmic reticulum-associated degradation. *Cell Reports* 2(6):1633–1644.
11. Mariappan M, et al. (2010) A ribosome-associating factor chaperones tail-anchored membrane proteins. *Nature* 466(7310):1120–1124.
12. Schuldiner M, et al. (2008) The GET complex mediates insertion of tail-anchored proteins into the ER membrane. *Cell* 134(4):634–645.
13. Wang Y, et al. (2014) GdX/UBL4A specifically stabilizes the TC45/STAT3 association and promotes dephosphorylation of STAT3 to repress tumorigenesis. *Mol Cell* 53(5): 752–765.
14. Krenciute G, et al. (2013) Nuclear BAG6-UBL4A-GET4 complex mediates DNA damage signaling and cell death. *J Biol Chem* 288(28):20547–20557.
15. Darlington GJ (1999) Molecular mechanisms of liver development and differentiation. *Curr Opin Cell Biol* 11(6):678–682.
16. Cross DA, Alessi DR, Cohen P, Andjelkovich M, Hemmings BA (1995) Inhibition of glycogen synthase kinase-3 by insulin mediated by protein kinase B. *Nature* 378(6559): 785–789.
17. Alessi DR, et al. (1996) Mechanism of activation of protein kinase B by insulin and IGF-1. *EMBO J* 15(23):6541–6551.
18. Oh WJ, et al. (2010) mTORC2 can associate with ribosomes to promote cotranslational phosphorylation and stability of nascent Akt polypeptide. *EMBO J* 29(23):3939–3951.
19. Xuan Nguyen TL, et al. (2006) Akt phosphorylation is essential for nuclear translocation and retention in NGF-stimulated PC12 cells. *Biochem Biophys Res Commun* 349(2):789–798.
20. Bijur GN, Jope RS (2003) Rapid accumulation of Akt in mitochondria following phosphatidylinositol 3-kinase activation. *J Neurochem* 87(6):1427–1435.
21. Pollard TD, Borisy GG (2003) Cellular motility driven by assembly and disassembly of actin filaments. *Cell* 112(4):453–465.
22. Rotty JD, Wu C, Bear JE (2013) New insights into the regulation and cellular functions of the ARP2/3 complex. *Nat Rev Mol Cell Biol* 14(1):7–12.
23. Spector I, Shochet NR, Kashman Y, Groweiss A (1983) Latrunculins: Novel marine toxins that disrupt microfilament organization in cultured cells. *Science* 219(4584):493–495.
24. Hetrick B, Han MS, Helgeson LA, Nolen BJ (2013) Small molecules CK-666 and CK-869 inhibit actin-related protein 2/3 complex by blocking an activating conformational change. *Chem Biol* 20(5):701–712.
25. Takenawa T, Suetsugu S (2007) The WASP-WAVE protein network: Connecting the membrane to the cytoskeleton. *Nat Rev Mol Cell Biol* 8(1):37–48.
26. Weisswange I, Newsome TP, Schleich S, Way M (2009) The rate of N-WASP exchange limits the extent of ARP2/3-complex-dependent actin-based motility. *Nature* 458(7234):87–91.
27. Campellone KG, Welch MD (2010) A nucleator arms race: Cellular control of actin assembly. *Nat Rev Mol Cell Biol* 11(4):237–251.
28. Ridley AJ, et al. (2003) Cell migration: Integrating signals from front to back. *Science* 302(5651):1704–1709.
29. Koestler SA, et al. (2013) Arp2/3 complex is essential for actin network treadmilling as well as for targeting of capping protein and cofilin. *Mol Biol Cell* 24(18):2861–2875.
30. Watton SJ, Downward J (1999) Akt/PKB localisation and 3′ phosphoinositide generation at sites of epithelial cell-matrix and cell-cell interaction. *Curr Biol* 9(8):433–436.
31. Xue G, Hemmings BA (2013) PKB/Akt-dependent regulation of cell motility. *J Natl Cancer Inst* 105(6):393–404.
32. Enomoto A, et al. (2005) Akt/PKB regulates actin organization and cell motility via Girdin/APE. *Dev Cell* 9(3):389–402.
33. Cenni V, et al. (2003) Targeting of the Akt/PKB kinase to the actin skeleton. *Cell Mol Life Sci* 60(12):2710–2720.
34. Xu W, et al. (2010) Integrin-induced PIP5K1C kinase polarization regulates neutrophil polarization, directionality, and in vivo infiltration. *Immunity* 33(3):340–350.
35. Klaunig JE, et al. (1981) Mouse liver cell culture. I. Hepatocyte isolation. *In Vitro* 17(10):913–925.
36. Pearce LR, Sommer EM, Sakamoto K, Wullschleger S, Alessi DR (2011) Protor-1 is required for efficient mTORC2-mediated activation of SGK1 in the kidney. *Biochem J* 436(1):169–179.
37. Zicha D, Dunn G, Jones G (1997) Analyzing chemotaxis using the Dunn direct-viewing chamber. *Methods Mol Biol* 75:449–457.
38. Zhang Y, et al. (2013) A network of interactions enables CCM3 and STK24 to coordinate UNC13D-driven vesicle exocytosis in neutrophils. *Dev Cell* 27(2):215–226.
39. Zhang Y, et al. (2010) Different roles of G protein subunits beta1 and beta2 in neutrophil function revealed by gene expression silencing in primary mouse neutrophils. *J Biol Chem* 285(32):24805–24814.